

Spherical stellarator with plasma current

Paul E. Moroz^{a)}

University of Wisconsin—Madison, Madison, Wisconsin 53706 and Lodestar Research Corporation, Boulder, Colorado 80301

(Received 27 February 1996; accepted 15 May 1996)

Recently proposed novel concept of a spherical stellarator (P. E. Moroz, "Spherical stellarator configuration," to appear in *Phys. Rev. Lett*) is enhanced by adding the plasma current to the otherwise pure stellarator system. The coil configuration of this ultra low aspect ratio system differs from that of a spherical tokamak by inclination of external parts of the toroidal field coils. It is shown that the configuration considered possesses many attractive properties, including: wide flexibility of operating regimes, compact design and coil simplicity, good access to the plasma, closed vacuum flux surfaces with large enclosed volume, significant external rotational transform, strong magnetic well, and a high plasma β [$\beta(0)$ in excess of 30%] equilibrium. It is shown that the bootstrap effect in a spherical stellarator, in principle, can supply the full plasma current required for the high- β equilibrium. © 1996 American Institute of Physics. [S1070-664X(96)03508-2]

I. INTRODUCTION

Continuous operation of a future thermonuclear reactor is probably absolutely necessary to make electricity production cost less than the other nonfusion methods. At the same time, the reactor has to be compact and as simple as possible (to keep construction and operation costs low), and have a modular design for convenient replacement of its part during exploitation in thermonuclear conditions. It has to be economical as well, which means operation at high β (β is the ratio of thermal plasma energy to the magnetic field energy).

Tokamaks and stellarators are presently two leading systems in the magnetic confinement fusion program. The largest devices for magnetic plasma confinement presently existing are tokamaks [the largest are the Joint European Torus (JET),¹ the Tokamak Fusion Test Reactor (TFTR),² and the Japan Tokamak (JT-60)³]. Tokamak operations with tritium plasmas carried out in TFTR² and JET¹ demonstrated significant fusion energy output. However, tokamaks are intrinsically pulsed devices, where pulse duration depends on the maximum magnetic flux produced by the Ohmic current transformer. For tokamak operation in a steady-state regime, significant additional power is required for current drive (CD) via neutral beam injection (NBI) or via rf techniques (RFCD). Regarding the fusion reactor, operation of these additional CD systems might increase significantly the total cost of electricity production. For a traditional pulsed tokamak-reactor scheme, there are also some other typical factors contributing to the cost increase, such as losses of the magnetic energy stored during the discharge, and the necessity for additional power required for the Ohmic transformer recharging.

There is, in principle, another approach to continuous tokamak operation: the ac regime in tokamaks.⁴⁻⁷ In this regime the Ohmic current direction is changed periodically. However, this regime can be fully beneficial only if the plasma is not lost at current reversal. Although the experiments on a small tokamak, STOR-1M,⁴ have been encourag-

ing and demonstrated an electron density of at least $2 \times 10^{12} \text{ cm}^{-3}$, similar experiments on a large tokamak, JET,⁵ found that plasma ionization was fully lost during the dwell time at current reversal. To enhance the ac regime of operation, the novel concept of a stellarator-tokamak hybrid called "stellamak"⁸⁻¹⁰ has been recently proposed. In a stellamak, the plasma can be confined during the current reversal phase via the stellarator properties of the device.

Another main type of devices for controlled nuclear fusion are stellarators,¹¹ which are intrinsically steady-state devices. Stellarators are presently somewhat behind in their development in comparison with tokamaks. Nevertheless, large stellarator devices are presently under construction in Japan [Large Helical Device (LHD)¹²] and in Germany [Wendelstein 7-X (W7-X)¹³]. Normally stellarators feature the large aspect ratio, $A \geq 10$. The projection of a standard stellarator to reactor parameters leads to a very large device with the major radius of around 25 m. Because the compact stellarator configuration is very attractive for a reactor design, a number of publications have addressed compact stellarator issues.¹⁴⁻¹⁸ The lowest aspect ratio stellarators ever built are the Compact Helical System (CHS)¹⁴ and the Compact Auburn Torsatron (CAT)¹⁵ which have $A \approx 5$. Even the stellarators with $A \approx 7.5$ such as the Advanced Toroidal Facility (ATF)^{19,20} or LHD are called¹⁶ low aspect ratio stellarators. Standard stellarators feature complicated (and difficult to accurately manufacture and assemble) helical windings or complicated sets of different three-dimensional coils (for the modular coil approach). Because of the relatively small distance between the neighboring coils, the plasma access in modular stellarators is also usually very limited. The accuracy of assembly has to be very high: Slight mistakes in the assembly can introduce significant island structures and disturbances to the magnetic surfaces. This is especially important problem for the relatively low aspect ratio stellarators.

Recently, strong interest has emerged for a very compact tokamak design, where a single central stack replaces the central parts of all toroidal coils. These low aspect ratio (LAR) tokamaks with $A = 1.5-2.5$ or ultra low aspect ratio (ULAR) tokamaks, with $A = 1.05-1.5$, are promising for ob-

^{a)}Electronic mail: moroz@engr.wisc.edu

taining plasma with a high number density and high β in a device of moderate size and relatively low magnetic field. Good plasma access is another advantage of these configurations. The LAR or ULAR tokamaks are also often called spherical tokamaks (ST). The first results reported from the spherical tokamaks. START (Small Tight Aspect Ratio Tokamak) at Culham^{21,22} and Current Drive Experiment-Upgrade CDX-U^{23,24} were very promising. In addition to the relatively high β obtained, low plasma disruptivity has been reported.^{21,24} Because of this initial success, the program on spherical tokamak is quickly extending and a number of proposals for construction of the new ST devices have appeared [for example, in the USA these are NSTX (National Spherical Tokamak Experiment),²⁵ USTX (University Spherical Tokamak Experiment),²⁶ and PEGASUS²⁷].

Some difficulties of the ST program are related to the fact that because of tight space for the Ohmic current transformer, it cannot support the inductive current for long time, and other noninductive current drive methods (such as RFCD or NBI) have to be used to maintain the plasma current beyond the initial Ohmic start-up. At the same time, as it is well known (see, for example, Refs. 25–29), that many standard rf current drive techniques, such as lower hybrid current drive (LHCD) or electron cyclotron current drive (ECCD), are problematic for the use in ST because of severe accessibility problems at the high plasma density and low magnetic field regimes typical for ST. The main noninductive CD methods presently proposed^{21–29} for ST are the neutral beam current drive (NBCD) and fast wave current drive (FWCD) at high ion cyclotron harmonic, $\omega \gg \Omega_{ci}$, regime (HHFW—high harmonic fast wave). Details of HHFW analysis have been presented in Ref. 28. Because of the low aspect ratio of ST, the trapped particle effects play a strong role, and both, NBCD and FWCD, although possible, are still difficult and tricky.

Another set of potential problems of the ST approach, as a next-step device or especially as a prototype for the fusion reactor, are related to the fact that there is not enough space, between the central stack and the plasma edge to protect the stack from the intense fluxes of heat, particles, and neutrons that can quickly damage the stack.

Recently, a similar LAR or ULAR approach has been proposed^{30,31} but, in contrast with the above mentioned tokamak systems, for stellarator configurations. Such stellarators have been called the spherical stellarators (SS) in analogy with the spherical tokamaks. In the SS devices considered, similar to that in ST, there was a single central stack replacing the internal parts of the toroidal field coils or helical coils of the standard stellarator. It was shown that the proposed systems possess many attractive properties including: very compact modular design and coil simplicity, good access to the plasma, closed vacuum flux surfaces with large enclosed volume, significant external rotational transforms, a strong magnetic well, and a simple toroidally symmetric divertor configuration. Moreover, it was found that in SS systems with a divertor, despite the ultra low aspect ratio, enough space is available between the central stack and the plasma surface to install a blanket and protect the stack from the intense fluxes of particles, heat and neutrons.

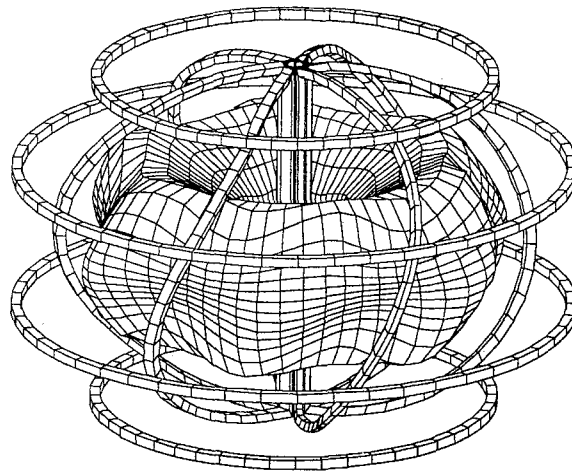


FIG. 1. Perspective view of a spherical stellarator (SS) with six TF coils. Shown are the coil system and the last closed flux surface.

The present paper can be viewed as an extension of our previous consideration^{30,31} of SS configurations to the regimes with plasma current. It was found that the addition of the plasma current improves some of the important features of SS. A high- β equilibrium [$\beta(0)$ in excess of 30%] in this system has been found as well, thus making the configuration considered a very attractive candidate for a future thermonuclear reactor. It is also shown that the strong bootstrap current in SS can fully support high- β equilibrium. While this paper was under review, further results have been obtained for LAR stellarator or tokamak–stellarator hybrid configurations.³²

The paper is organized as follows. In Sec. II, the coil configuration and the magnetic field properties of the SS system are presented briefly. The difference from the SS system considered here and presented in Refs. 30 and 31 is that there the results for a configuration with the divertor coils were given. Here, we do not address the subject of a divertor but instead focus on the effects of the plasma current. In Sec. III, many unusual features of the SS magnetic field structure are discussed. In Sec. IV, the effects of the plasma current on the magnetic field configuration in SS are presented. Plasma equilibrium with the current is calculated via the VMEC code.^{33–35} The high- β equilibrium properties of SS are demonstrated as well. In Sec. V, the effects of the bootstrap current in SS are presented. Finally, the discussion and main conclusions are given in Sec. VI.

II. THE COIL SYSTEM OF A SPHERICAL STELLARATOR

The SS device, as it was proposed in Refs. 30 and 31, can be obtained from the corresponding ST configuration by rotating the top parts of the toroidal field (TF) coils relative to their bottom parts, over the toroidal angle $\Delta\varphi$. Thus the external parts of the modified TF coils are inclined (see Fig. 1). Good results were obtained for $\Delta\varphi = \pi/N$, where N is the number of TF coils in ST. In some sense, this type of SS configuration is similar to a device with inclined coils de-

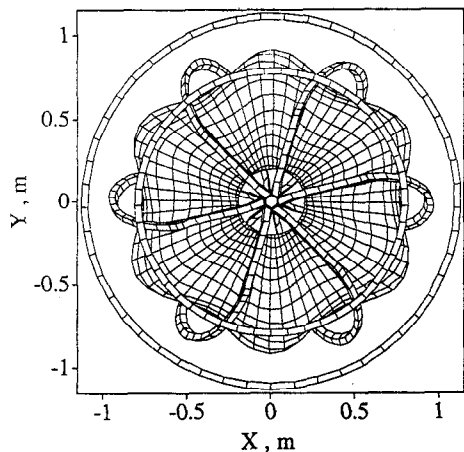


FIG. 2. Same as Fig. 1 but the top view is given.

scribed in our recent publications,^{8-10,36} but corresponds to the ultra low aspect ratio. Similar to a device with inclined coils, the SS of the type considered requires a set of poloidal field (PF) coils to compensate for the vertical magnetic field produced by the inclined parts. The SS configuration with six TF coils (modified as described above) is shown in Fig. 1. The last closed flux surface can be seen as well. The top view of SS is given in Fig. 2. As in any other stellarator, the magnetic flux surfaces in SS are three-dimensional (3-D). The vertical cross section of the device and the last closed flux surface are presented in Fig. 3. The coil projections are given, so that the particular dimensions, chosen for this example, can be readily seen. Three different cross sections for the last closed flux surface are shown: at toroidal angles $\varphi=0$ (solid curve), $\pi/2N$ (dash), π/N (dot-dash). Toroidal angle $\varphi=0$ corresponds to the cross section where the outboard inclined part of the TF coil crosses the equatorial plane.

We use the following definition of the plasma aspect ratio in SS: $A = (R_{\max} + R_{\min})/2\rho_{\max}$, where $\rho_{\max} = \langle r_p \rangle$. Here, a symbol $\langle \rangle$ means averaging over the poloidal, ϑ , and toroidal, φ , angles. The value of $r_p(\vartheta, \varphi)$ is the minor radius on the last closed flux surface for given (ϑ, φ) , and R_{\max} , R_{\min} are the maximum and minimum major radii

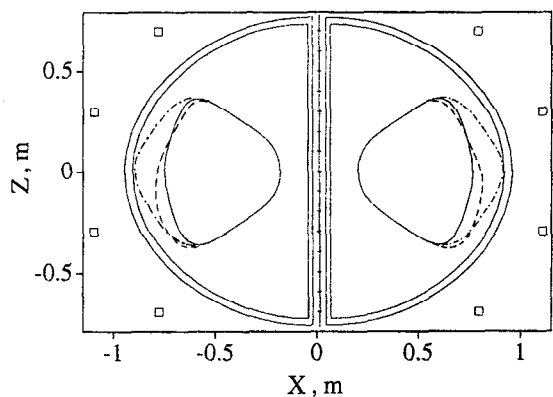


FIG. 3. Vertical cross-section of the SS device of Fig. 1. Shown are the coil projections and the cross sections for the last closed flux surface at toroidal angles $\varphi=0$ (solid curve), $\pi/2N$ (dash), and π/N (dot-dash).

for the last closed flux surface. Our definition of aspect ratio, A , is somewhat different from its usual definition used by the stellarator community. Usually, the plasma aspect ratio, A_p , is defined (see, for example, Ref. 16) by the relation, $A_p = R_0/\langle r_p \rangle$, where R_0 is the major radius of the helical field winding. For SS, R_0 should be replaced, probably, by the average major radius of the TF coil. The parameter, A_p , is not convenient for use in SS, because the plasma location can be significantly different (near the central stack, or in the opposite case, at larger major radii, near the inclined parts of the TF coils) but still have the same $\langle r_p \rangle$, and hence, the same A_p .

III. MAGNETIC FIELD PROPERTIES OF A SPHERICAL STELLARATOR

Spatial variation of the magnetic field strength, $|B|$, is of importance for plasma confinement as well as auxiliary plasma heating in a device. In a tokamak, $|B|$ mainly depends only on the major radius, and does not depend on the toroidal angle, φ . Thus the $|B|$ contour lines are close to the vertical lines. In a stellarator with a strong helical component, a saddle point of $|B|$ appears in the poloidal cross section (see, for example, Ref. 37). The behavior of $|B|$ in SS combines features of a tokamak and a stellarator.

Closed vacuum magnetic flux surfaces calculated for SS by the field line tracing are shown in Fig. 4 for different poloidal cross sections at toroidal angles: $\varphi=0$, $\varphi=\pi/2N$, and $\varphi=\pi/N$. All flux surfaces are presented by their Poincaré plots, except the last closed flux surface where the neighboring points are connected, to make the boundary more clearly visible. One can see that it is convenient to divide each flux surface into two parts—the external (outboard) and internal (inboard). The internal parts of the flux surfaces do not change their shape with the change of the toroidal angle, which is a typical characteristic of a tokamak. By contrast, the external parts change significantly with the toroidal angle, similar to a typical stellarator.

Similar combination of the tokamak and stellarator features can be seen in Fig. 5 showing $|B|$ distribution in the poloidal cross section, again, at different toroidal angles: $\varphi=0$, $\varphi=\pi/2N$, and $\varphi=\pi/N$. At small major radii, the $|B|$ contours are given by the vertical lines and do not depend substantially on the toroidal angle, similar to a tokamak, but at the larger major radii, $|B|$ has clear stellarator features: $|B|$ varies significantly with the toroidal angle and has a saddle point at the $\varphi=0$ cross section.

Variation of $|B|$ on a given flux surface and along the magnetic field line is of primary interest for particle transport analysis.³⁸⁻⁴¹ Although we do not present the transport analysis here, the distributions of $|B|$ along field lines and on given flux surfaces are shown in Figs. 6 and 7, respectively, for the last closed flux surface, $\rho=\rho_{\max}$, the middle flux surface at $\rho=0.5\rho_{\max}$, and the flux surface near the magnetic axis, $\rho=0.05\rho_{\max}$.

From Fig. 6(c) one can see that, near the magnetic axis ($\rho=0.05\rho_{\max}$), the leading harmonics, with $n=6$ (corresponding to the number of TF coils) are much stronger than the toroidally symmetrical harmonic with $m=1$, $n=0$. Here, m and n are, respectively, the poloidal and toroidal mode num-

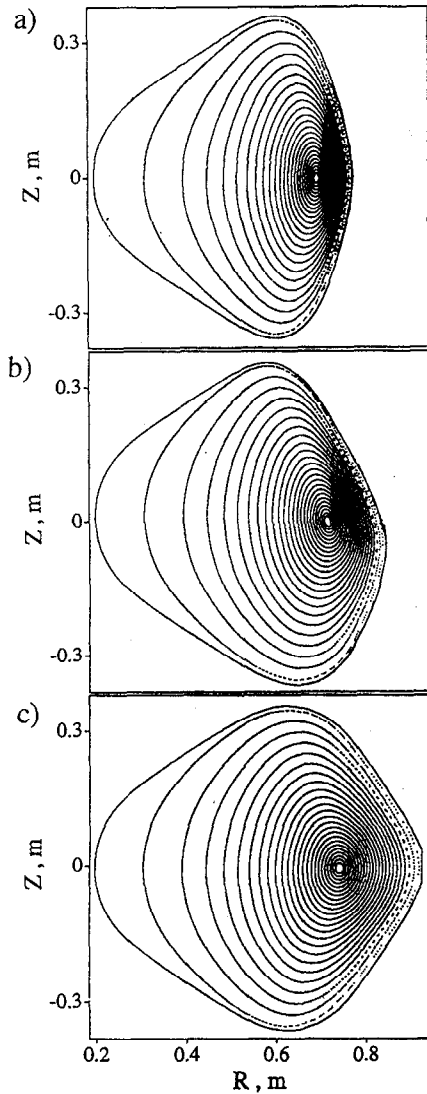


FIG. 4. Vacuum flux surfaces in SS at different cross sections. (a) $\varphi=0$, (b) $\varphi=\pi/2N$, (c) $\varphi=\pi/N$. All flux surfaces are presented by their Poincaré plots, except the last closed flux surface where the neighboring points are connected.

bers. This is a typical result for a stellarator with a helical magnetic axis. By contrast, for the last flux surface, $\rho=\rho_{\max}$ [Fig. 6(a)], the toroidal harmonics with $n=0$ are stronger than other harmonics, and $|B|$ variation is close to that in a tokamak. The case of $\rho=0.5\rho_{\max}$ corresponds to the intermediate case when toroidal and helical harmonics are the same order of magnitude [Fig. 6(b)].

Variation of $|B|$ on a flux surface, presented in Fig. 7, stresses the same features. Near the magnetic axis [Fig. 7(c)] the $n=6$ harmonics are strongest. By contrast, for the last close flux surface, $\rho=\rho_{\max}$ [Fig. 7(a)], there is weak dependence of $|B|$ on the toroidal angle (similar to that in a tokamak) on the high field side of the flux surface (where $0.3 < \vartheta/2\pi < 0.7$). It is interesting to note that at the outboard (stellarator) parts of flux surfaces (where $0 < \vartheta/2\pi < 0.2$, or $0.8 < \vartheta/2\pi < 1$) the $|B|$ contours are well represented by straight lines with definite slope. This feature corresponds to the so-called helically symmetric stellarator configuration,

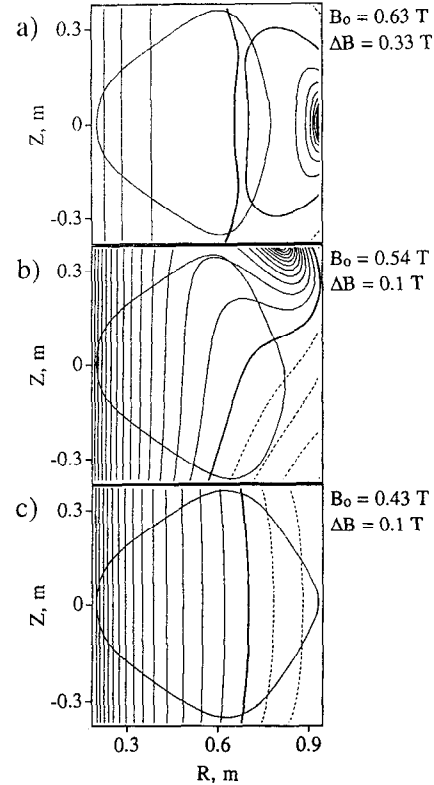


FIG. 5. Distribution for $|B|$ for different poloidal cross sections: (a) $\varphi=0$, (b) $\varphi=\pi/2N$, (c) $\varphi=\pi/N$. The value of B_0 corresponds to the bold curve, ΔB is the difference between the adjacent corner lines. Solid lines correspond to $|B| > B_0$, and dashed to $|B| < B_0$. The last closed flux surface is shown as well.

normally featuring good confinement properties.^{13,42,43}

Variation of $|B|$ along field lines is often characterized also by the magnetic field modulation: $\eta(\rho) = (B_{\max} - B_{\min}) / (B_{\max} + B_{\min})$. The radial dependence of $\eta(\rho)$ for the device considered is presented in Fig. 8(a) by the dashed curve. One can see that η is a growing function of ρ , and $\eta_{\max} \approx 67\%$ at the outermost flux surface with $\rho \approx 29$ cm. This value of the field modulation, although large, is still less than that in a typical ST device.

The magnetic configuration of SS is favorable to magnetohydrodynamic (MHD) stability. It possesses a strong magnetic well, which can be defined through the integral, $U = \int dl/B$, taken along the field line and averaged over the flux surface. The average of the integral U can be expressed through the derivative of the enclosed volume, V , over the enclosed toroidal magnetic flux Φ :⁴⁴ $\langle U \rangle = dV/d\Phi$. The magnetic configuration is favorable to MHD stability if $\langle U \rangle$ decreases with the average minor radius, ρ . The relative deepness of the magnetic well can be defined as $W(\rho) = 1 - \langle U(\rho) \rangle / \langle U(0) \rangle = 1 - V'(\Phi(\rho)) / V'(0)$, where $U(0)$ and $V'(0)$ correspond to the values at the magnetic axis, and $U(\rho)$ and $V'(\Phi(\rho))$ to the values at the given flux surface with the average minor radius, ρ . Figure 8(a) shows (solid curve) the dependence of $W(\rho)$, that corresponds to a total magnetic well of about $W_i = 61\%$. This is a very high number, ensuring the good stability properties of the SS configuration.

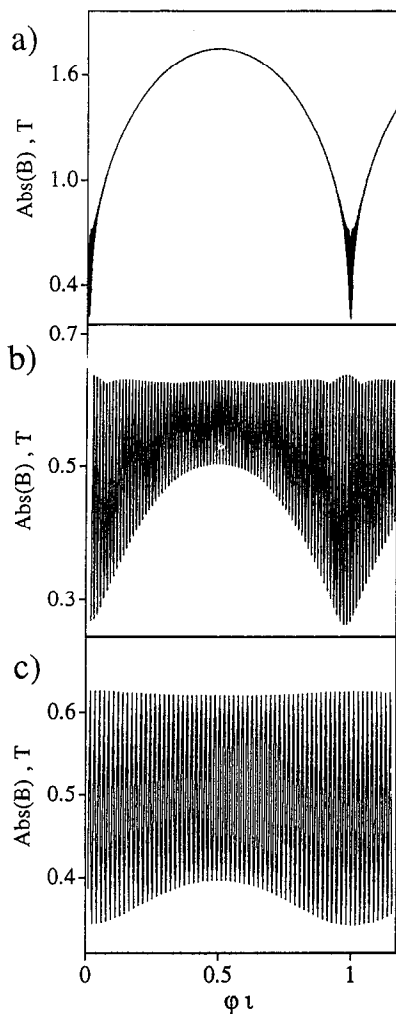


FIG. 6. Variation of $|B|$ along field line for different flux surfaces: (a) $\rho = \rho_{\max}$, (b) $\rho = 0.5\rho_{\max}$, (c) $\rho = 0.05\rho_{\max}$.

Rotational transform behavior in SS is very different from that in a typical stellarator. Figure 8(b) shows the radial dependence of the rotational transform, $\iota = 1/q$, q being the safety factor, for the device shown in Fig. 1. As one can see, the total rotational transform, ι (solid curve), is a decreasing function of ρ , which is typical for tokamaks and is very rare in stellarators. In SS, the local ι changes significantly in the poloidal direction: it is relatively large [dashed curve in Fig. 8(b), showing increasing ι_{ex} with ρ] on the external (outboard) halves of the flux surfaces, which are closer to the inclined parts of the TF coils, and small on the internal (inboard) halves of the flux surfaces (dotted curve, for ι_{in}). The relation between the total ι and its external, ι_{ex} , and internal, ι_{in} , components can be expressed as: $2/\iota \approx 1/\iota_{\text{ex}} + 1/\iota_{\text{in}}$. The relatively large value of the local outboard rotational transform ι_{ex} and the corresponding shear are of importance for good plasma stability properties in SS.⁴⁵

Addition of the finite plasma pressure and/or plasma current changes the magnetic flux surface configuration significantly. To study the three-dimensional equilibria in SS, including cases with the plasma current (which is also three-dimensional), we have used the VMEC code³³⁻³⁵ running in

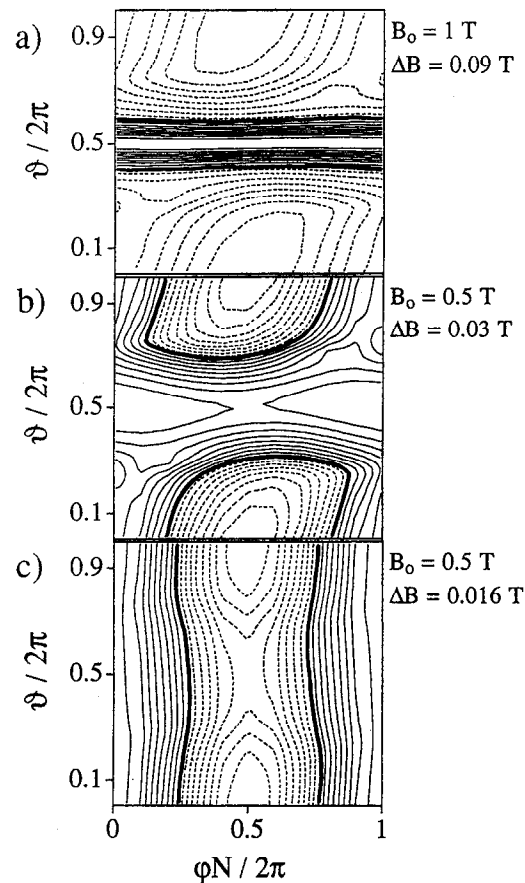


FIG. 7. Distribution of $|B|$ on different flux surfaces: (a) $\rho = \rho_{\max}$, (b) $\rho = 0.5\rho_{\max}$, (c) $\rho = 0.05\rho_{\max}$. The value of B_0 corresponds to the medium value, ΔB is the difference between the adjacent contour lines. Solid contour lines correspond to $|B| \geq B_0$, and dashed to $|B| < B_0$.

the free boundary mode. It is very important to use this mode of computation because the plasma boundary shape and plasma location depend significantly on the plasma current and/or plasma β .

Normally, with increase of the plasma β , an additional vertical magnetic field is required for plasma equilibria. In our calculations, the same set of four PF coils, used for obtaining the vacuum flux surfaces, was also used for obtaining the finite β equilibria (or equilibria with the plasma current). The currents of the PF coils, however, were different from that for the vacuum case. An example of the currentless case with $\langle\langle\beta\rangle\rangle = 1\%$ (double brackets, $\langle\langle \rangle\rangle$, mean volume averaging) is given in Fig. 9. One can see that the plasma became much more vertically elongated. This feature becomes more and more profound with the increase of β , thus setting a β limit on plasma pressure for the currentless case.

It is worth mentioning, however, that consideration of the currentless regimes in SS for high β cases is not realistic. The strong bootstrap current appears in SS at high β (see Sec. V), thus converting SS into a device with plasma current.

IV. HIGH- β REGIMES WITH PLASMA CURRENT

During analysis of the SS configuration considered, it was found that its properties improve with the addition of

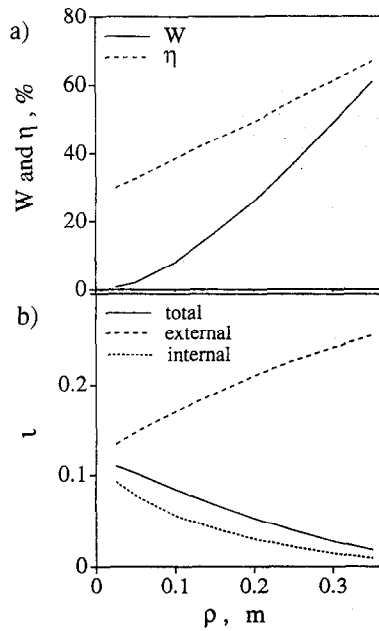


FIG. 8. Radial dependence of a few important parameters in SS for a vacuum case: (a) the magnetic well, W , and the magnetic field variation, η ; (b) the total rotational transform (solid curve) and its external (dashed), and internal (dotted) components.

plasma current. This is opposite to the standard stellarator configuration, where addition of the Ohmic plasma current or even a small bootstrap current degrades the system, and special efforts are needed to find the configuration with the smallest bootstrap current possible (see, for example, Refs. 46 and 47).

To demonstrate the high β equilibrium properties of the SS system considered, we present results for a high pressure plasma. The plasma density and electron and ion temperature profiles were suggested to be parabolic: $n_e(\rho)/n_e(0) = T_e(\rho)/T_e(0) = T_i(\rho)/T_i(0) = 1 - (\rho/\rho_{\max})^2$. The plasma current of $I_p = 200$ kA was flowing in the direction such that the Ohmic rotational transform and vacuum rotational transform add constructively. The current density profile was chosen to be parabolic as well. One can see that the plasma shape for the case with the plasma current is very different from the currentless case presented above. The total rotational transform has changed as well. It has increased to $\iota(0) \approx 0.74$ at the axis and $\iota(\rho_{\max}) \approx 0.25$ at the plasma edge.

The case, presented in Fig. 10, corresponds to the high- β plasma equilibrium, with the central value of $\beta(0) = 33\%$ ($\langle\langle\beta\rangle\rangle \approx 9\%$). It is important to note that this very high value of β is not a limit for SS. We did not try to find the maximum or limiting β for equilibrium. However, the case presented shows clearly that very high β can be reached in the SS systems.

It should be mentioned also, that a strong magnetic well ($W_i \approx 70\%$) exists in the high β case of Fig. 10. This is a very favorable situation for good plasma stability.

Previous analysis of β limits, made for the low aspect ratio stellarators (see, for example, Ref. 18), shows that they are defined by the MHD equilibrium and not stability. Hence,

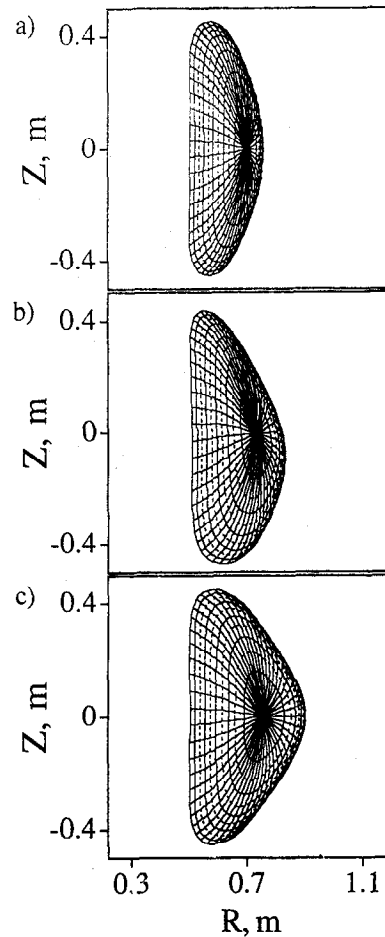


FIG. 9. Currentless equilibrium in SS calculated by the vmec code (in its free-boundary mode) for the case of $\langle\langle\beta\rangle\rangle=1\%$. Different cross-sections are shown: (a) $\varphi=0$, (b) $\varphi=\pi/2N$, (c) $\varphi=\pi/N$.

it is likely, that the high equilibrium- β regimes found for SS, will be really accessible. Still, more detailed calculations regarding the plasma stability at high β are necessary to fully confirm this conclusion for SS.

One more advantage of adding the plasma current to the system is that the plasma with current can be easily moved horizontally by changing the vertical magnetic field (by changing the currents in the PF coils). As a particular case, the typical plasma configuration for the ST device touching the central stack can be obtained simply by increasing the vertical magnetic field. Our calculations show, however, that the stellarator features decrease substantially with the plasma moving closer to the central stack. The plasma becomes almost toroidally symmetric and the total rotational transform decreases by the value approaching the vacuum rotational transform.

That means that SS can be operated in the regimes similar to that in ST. Normally, SS can be operated with the smaller plasma currents than the corresponding ST; still, SS might have similar rotational transform (or the safety factor) as the corresponding ST. If the plasma current needs to be driven externally, then one can save significantly on the re-

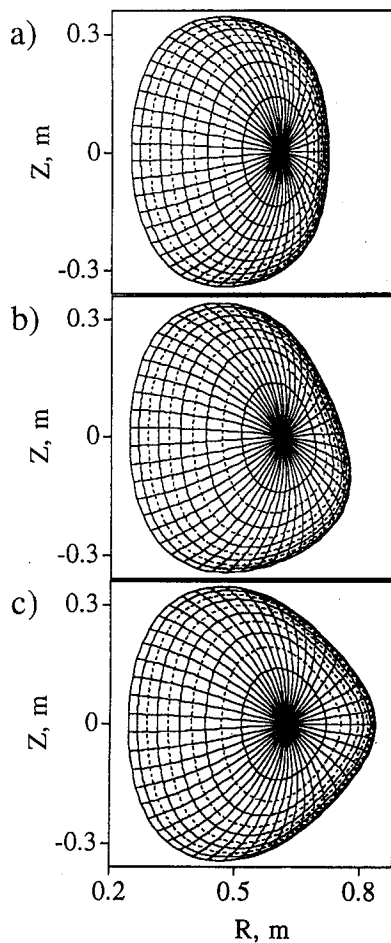


FIG. 10. Magnetic flux surfaces for the high- β plasma ($\beta(0)=33\%$) in SS with the plasma current of 200 kA: (a) $\varphi=0$, (b) $\varphi=\pi/2N$, (c) $\varphi=\pi/N$.

quired auxiliary current drive systems necessary for continuous operation of the device.

The SS with plasma current, has a wide flexibility of changing the plasma configuration from one having strong stellarator features to the other, typical for the toroidally symmetric ST device.

V. STRONG BOOTSTRAP CURRENT IN SS

The bootstrap current⁴⁸ in tokamaks represents a powerful mechanism of the passive current drive by the plasma pressure gradient. The principal possibility of a steady-state tokamak relies on a substantial portion of the bootstrap current. Still in a tokamak, the bootstrap current cannot drive the full plasma current, and significant auxiliary current drive by neutral beam injection or radio-frequency waves is necessary.

In contrast to that, in stellarators, the bootstrap current appears by itself and does not need any seed current. It also can be positive or negative. However, usually the bootstrap current in stellarators causes many problems by changing the rotational transform profile with the increase of plasma pressure. As a result, many efforts have been made (see, for

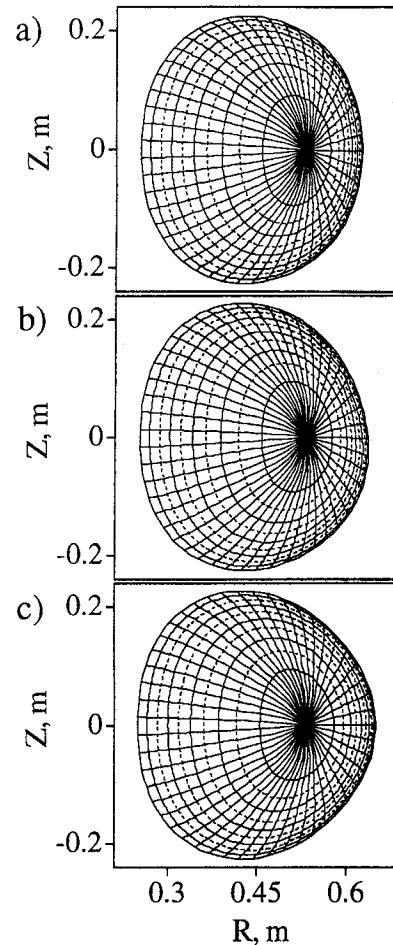


FIG. 11. Equilibrium in SS for the same high- β plasma as presented in Fig. 9 but for the case with the hollow current profile produced by the bootstrap effect alone: (a) $\varphi=0$, (b) $\varphi=\pi/2N$, (c) $\varphi=\pi/N$.

example, Refs. 46 and 47) to search for the stellarator configurations with substantially minimized bootstrap current.

For the SS devices considered at high β , our calculations show rather significant bootstrap current flowing in such a direction that the current rotational transform enhances the vacuum rotational transform. Strong bootstrap current, I_{bs} , is advantageous for SS and improves the whole concept.

Our calculations of the bootstrap current in SS are based on a few codes written at the Oak Ridge National Laboratory: the VMEC code mentioned above and used for the 3-D equilibrium calculations; the code converting VMEC results to Boozer coordinates; and the BOOTSJ code⁴⁹⁻⁵¹ for the bootstrap current calculations. Final results for the bootstrap current are used then as input data for the VMEC code for the next iteration. The codes are modified to work successively one after another and special steps are taken to improve the convergence process. Details of such calculations represent a subject for a separate paper and will be discussed elsewhere. Somewhat similar calculations for the LHD stellarator were carried out in Ref. 52. Here, we show just a few results, obtained for the SS device with the same parameters as considered above.

Figure 11 shows the final plasma equilibrium with the

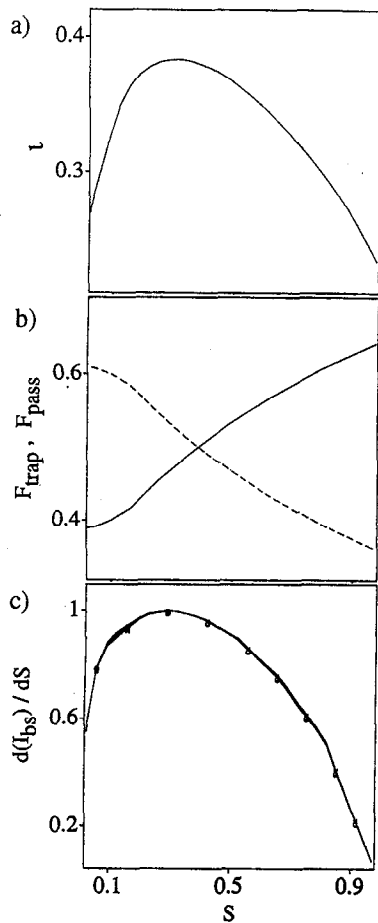


FIG. 12. A few important characteristics of the high- β equilibrium in SS corresponding to Fig. 11; (a) radial variation of the total rotational transform. (b) fraction of trapped (solid curve) and passing (dashed) particles. (c) the bootstrap current density profile.

bootstrap current, found for the same parabolic profiles of plasma density and temperature, and almost the same high β values of the plasma, as in the previous case of Fig. 10. The plasma current profile is, however, substantially different and is defined fully by the bootstrap current alone.

The total rotational transform, ι , is presented in Fig. 12(a). The fraction of trapped, F_{trap} , and passing, F_{pass} , particles important for the bootstrap current calculations, is given in Fig. 12(b), while the bootstrap current density is shown in Fig. 12(c). The total bootstrap current was found to be 170 kA. Three curves in Fig. 12(c), close to each other, demonstrate the convergence process; they show results of the last two iterations and the intermediate curve chosen as the final result. The relative error for the calculated profile is less than 1%. The radial variable, s , represents the normalized enclosed toroidal flux: $s = \Phi/\Phi_{\text{max}}$.

VI. DISCUSSION AND CONCLUSIONS

A recently proposed³⁰⁻³³ novel configuration of a spherical stellarator (SS) is further analyzed in this paper to present the effects of the plasma current on the magnetic field structure and equilibrium properties.

It is found that the plasma current flowing in the direction such that its rotational transform adds constructively to the stellarator rotational transform, produced by the inclined parts of the TF coils, makes the following positive changes to the configuration.

- (i) total rotational transform increases in comparison with the currentless case;
- (ii) horizontal plasma position can be effectively controlled by the currents in the PF coils;
- (iii) magnetic axis location can be effectively controlled to produce more symmetric positioning;
- (iv) very high- β equilibria [$\beta(0) > 30\%$] exist (the limiting β is likely to be even larger);
- (v) the strong magnetic well (70% for the case considered) exists in the SS configuration with the high β and plasma current. This should improve the plasma stability properties.

These positive results of the plasma current effects are in strong contrast to what have been found for standard stellarator systems, where addition of the Ohmic plasma current or even a small bootstrap current degrades the system, and special efforts are needed to find the configuration with the smallest plasma current possible.

The SS system considered thus can be effectively operated with plasma current. In the case where the plasma current is provided by the Ohmic current transformer, one will have a hybrid stellarator-tokamak device, that can, probably, also be called a "Spherical Tokamak with Twisted Coils" (STTC). This hybrid device might have a number of advantages over the standard ST. The plasma discharge in STTC can be started in the pure stellarator regime without plasma current. Then, when the relatively dense and hot plasma is obtained via the auxiliary heating methods, the plasma current can be effectively induced by the Ohmic current transformer. Then the plasma can be moved inside closer to the central stack by changing the currents in the PF coils to form the standard very low aspect ratio configuration of a spherical tokamak. This method of plasma start-up might save significant magnetic flux which is usually very limited in ST because of lack of space for the large Ohmic current transformer.

Other alternatives for supplying the plasma current in SS can be the plasma current via the standard external current drive (via neutral beam injection or rf current drive) or via the bootstrap current effects. In that case, SS has a lot of advantages over ST because it does not need as much current to drive as a ST. Also in that case, SS does not need the Ohmic current transformer, and can be operated continuously in the regime with the plasma current.

In this paper, it is shown also that the bootstrap current is rather significant in SS at high β and is flowing in such a direction that the current rotational transform enhances the vacuum rotational transform. Availability of the bootstrap current enhances the whole SS concept. Consideration of the currentless regimes in SS is thus irrelevant to the high β plasmas. A particular example is presented in this paper to demonstrate that the high β equilibrium exists with the full plasma current produced by the bootstrap effect alone.

A relatively small SS device has been considered in the numerical examples presented in this paper. Such a device is probably relevant to the first university-scale proof-of-principle experiment. Plasma confinement characteristics cannot be very good in such a relatively small device. This fact will set a limit on the accessible β values. Still, the main stellarator characteristics of SS and first experience on the following questions important for this concept can be obtained: plasma start-up in SS, position control, divertor operation, effects of the Ohmic plasma current, and transition between the stellarator regimes, when the plasma is located near the inclined parts of the coils, and the ST regimes, when the plasma position is very close to the central stack. First experimental information on the effects of the stellarator characteristics on the operation of SS with the plasma current will be valuable as well. Because the plasma current is important for the whole SS concept, and the current cannot be fully supported by the bootstrap effect alone in a relatively small device, the Ohmic current transformer has to be a part of such an initial experiment.

Our future work will include the analysis of the plasma transport characteristics in SS. This will let us define the critical size of the device necessary for obtaining the high- β plasma with the full plasma current produced by the bootstrap effect alone at the reasonable input power levels required for plasma heating. The second step in the experimental program on SS might be, then, construction of a relatively large device where the bootstrap effect alone can support the high- β operation. Such a large device can be designed to operate in steady-state without using the Ohmic current transformer.

Transfer of the results described in this paper to the larger device is straightforward. One just has to take into account the following scaling laws, partially discussed in Ref. 36. If the size of all current carrying elements is increased by the same factor, C , then the flux surface geometry and location of flux surfaces relative to the coils will be similar. To keep the same value of the magnetic field, however, will require the increase of all currents by the same factor, C . The similar plasma density and temperature profiles and the same central values will then produce similar β profiles. The total bootstrap current will increase by the same factor, C , thus the ratio of the bootstrap current to the current in the coil elements will stay the same.

The analysis of SS configurations made so far shows many unusual features and clear indications of many possible advantages of SS over the other "standard" configurations for magnetic plasma confinement. Further studies of SS are in progress.

ACKNOWLEDGMENTS

The author is thankful to Gilbert Emmert, Noah Hershkowitz, James Callen, Joseph Talmadge, and David Anderson for useful discussions. Cooperation of Steve Hirshman in making the VMFC code available and his help and valuable instructions are greatly appreciated. The author would like also to acknowledge S. P. Hirshman, J. S. Tolliver, D. K. Lee,

and K. C. Shaing for providing the original numerical codes for the conversion to Boozer coordinates and for the bootstrap current calculation.

This work was supported by the U.S. Department of Energy Grants No. DE-FG02-88ER53264 and No. DE-FG02-88ER53263.

- ¹J. Jacquinot and the JET Team, *Plasma Phys. Controlled Fusion* **35**, A35 (1993).
- ²R. J. Hawryluk and the TFTR Team, in *Proceedings of the 15th International Conference on Plasma Physics and Controlled Nuclear Fusion Research*, Seville, 1994 (International Atomic Energy Agency, Vienna, 1995), Vol. 1, p. 11.
- ³M. Kikuchi and the JT-60 Team, in Ref. 2, p. 31.
- ⁴O. Mitarai, S. W. Wolfe, A. Hirose, and H. M. Skarsgard, *Nucl. Fusion* **27**, 604 (1987).
- ⁵B. Tubbing, B. Green, J. How, M. Huart, P. Kupschus, P. Lallia, P. Lomas, C. Lowry, P. Noll, P. H. Rebut, D. Stork, A. Tanga, A. Taroni, and T. Wijnands, *Bull. Am. Phys. Soc.* **36**, 2365 (1991).
- ⁶O. Mitarai, S. W. Wolfe, A. Hirose, and H. M. Skarsgard, *Fusion Technol.* **15**, 204 (1989).
- ⁷O. Mitarai, A. Hirose, and H. M. Skarsgard, *Fusion Technol.* **20**, 285 (1991).
- ⁸P. E. Moroz, *Proceedings 22nd EPS Conference, Controlled Fusion and Plasma Physics*, Bournemouth, UK (European Physical Society, Petit-Lancy, Switzerland, 1995), Vol. 19C, p. II-049.
- ⁹P. E. Moroz, *Bull. Am. Phys. Soc.* **40**, 1858 (1995).
- ¹⁰P. E. Moroz, "Stellarator-tokamak hybrid with inclined coils," to appear in *Fusion Technol.* (September 1996).
- ¹¹J. F. Lyon, *Fusion Technol.* **17**, 19 (1990).
- ¹²A. Iiyoshi, M. Fujiwara, O. Motojima, N. Ohyanu, and K. Yamazaki, *Fusion Technol.* **17**, 169 (1990).
- ¹³C. Beidler, G. Grieger, F. Herrnegger, E. Harneyer, J. Kisslinger, W. Lotz, H. Maassberg, P. Merkel, J. Nuhrenberg, F. Rau, J. Sapper, F. Sardei, R. Scardovelli, A. Schluter, and H. Wobig, *Fusion Technol.* **17**, 148 (1990).
- ¹⁴K. Nishimura, K. Matsuoka, M. Fujiwara, K. Yamazaki, J. Todoroki, T. Kamimura, T. Amano, H. Sanuki, S. Okamura, M. Hosokawa, H. Yamada, S. Tanahashi, S. Kubo, Y. Takita, T. Shoji, O. Kaneko, H. Iguchi, and C. Takahashi, *Fusion Technol.* **17**, 86 (1990).
- ¹⁵S. F. Knowlton, R. F. Gandy, J. D. Hanson, G. J. Hartwell, and H. Lin, *J. Fusion Energy* **12**, 261 (1993).
- ¹⁶J. F. Lyon, B. A. Carreras, V. E. Lynch, J. S. Tolliver, and I. N. Sviatovskiy, *Fusion Technol.* **15**, 1401 (1989).
- ¹⁷B. A. Carreras, N. Dominguez, L. Garcia, V. E. Lynch, J. F. Lyon, J. R. Cary, J. D. Hanson, and A. P. Navarro, *Nucl. Fusion* **28**, 1195 (1988).
- ¹⁸J. F. Lyon, B. A. Carreras, N. Dominguez, L. Dresner, C. L. Hedrick, S. P. Hirschman, M. S. Lubell, J. W. Lue, R. N. Morris, S. L. Painter, J. A. Rome, and W. I. Rij, *Fusion Technol.* **17**, 188 (1990).
- ¹⁹J. F. Lyon, B. A. Carreras, K. K. Chipley, M. J. Cole, J. H. Harris, T. C. Jernigan, R. L. Johnson, V. E. Lynch, B. E. Nelson, J. A. Rose, J. Sheffield, and P. B. Thompson, *Fusion Technol.* **10**, 179 (1986).
- ²⁰J. F. Lyon, G. L. Bell, J. D. Bell, R. D. Benson, T. S. Bigelow, K. K. Chipley, R. J. Colchin, M. J. Cole, E. C. Crume, J. L. Dunlap, A. C. England, J. C. Glowienka, R. H. Goulding, J. H. Harris, D. L. Hillis, S. Hiroe, L. D. Horton, H. C. Howe, R. C. Isler, T. C. Jernigan, R. L. Johnson, R. A. Langley, M. M. Menon, P. K. Mioduszewski, R. N. Morris, M. Murakami, G. H. Neilson, B. E. Nelson, D. A. Rasmussen, J. A. Rome, M. J. Saltmarsh, P. B. Thompson, M. R. Wade, J. A. White, T. L. White, J. C. Whitson, J. B. Wilgen, and W. R. Wing, *Fusion Technol.* **17**, 33 (1990).
- ²¹A. Sykes, M. Bevir, R. A. Bamford, R. J. Colchin, R. Duck, S. K. Ereints, J. Ferreira, K. Gibson, C. G. Gimblett, D. H. J. Goodall, M. Gryaznevich, T. C. Hender, J. Hugill, I. Jenkins, R. Martin, S. Parry, C. Ribeiro, D. C. Robinson, N. Sakharov, J. Thomas, M. F. Turner, M. J. Walsh, and H. R. Wilson, in *Proceedings of the 15th International Conference on Plasma Physics and Controlled Fusion Research*, Seville, 1994 (International Atomic Energy Agency, Vienna, 1995), Vol. 1, p. 719.
- ²²M. Gryaznevich, J. Hugill, I. Jenkins, R. Martin, A. Sykes, and M. J. Walsh, *Bull. Am. Phys. Soc.* **40**, 1656 (1995).
- ²³M. Ono, C. B. Forest, Y.-S. Hwang, R. J. Armstrong, W. Choe, D. S. Darrow, G. J. Greene, T. Jones, T. R. Jarboe, A. Martin, B. A. Nelson, D. Orvis, C. Painter, L. Zhou, J. A. Rogers, M. J. Schaffer, A. W. Hyatt, R. I. Pinsker, G. M. Staebler, R. D. Stambaugh, E. J. Strait, K. L. Greene, J. A.

- Leuer, and J. M. Lohr, in *Proceedings of the International Conference on Plasma Physics and Controlled Fusion Research*, Würzburg, 1992 (International Atomic Energy Agency, Vienna, 1993), Vol. 1, p. 693.
- ²⁴Y. S. Hwang, M. Yamada, T. G. Jones, M. Ono, W. Choe, S. C. Jardin, E. Lo, G. Ludwig, J. Menard, A. Fredriksen, R. Nazikian, N. Pomphrey, S. Yoshikawa, A. Morita, Y. Ono, T. Itagaki, M. Katsurai, and K. Tokimatsu, in *Proceedings of the 15th International Conference on Plasma Physics and Controlled Fusion Research*, Seville, 1994 (International Atomic Energy Agency, Vienna, 1995), Vol. 1, p. 737.
- ²⁵M. Ono, R. Goldston, S. Kaye, Y.-K. M. Peng, and the NSTX Team, *Bull. Am. Phys. Soc.* **40**, 1655 (1995).
- ²⁶The USTX Team (University of Texas at Austin, private communication, 1995).
- ²⁷R. J. Fonck, R. Durst, T. Intrator, G. Garstka, C. Hegna, and K. Tritz, *Bull. Am. Phys. Soc.* **40**, 1656 (1995).
- ²⁸M. Ono, *Phys. Plasmas* **2**, 4075 (1995).
- ²⁹J. Robertson, R. Majeski, J. Menard, M. Ono, and J. R. Wilson, *Bull. Am. Phys. Soc.* **40**, 1655 (1995).
- ³⁰P. E. Moroz, "Spherical stellarator configuration," to appear in *Phys. Rev. Lett.*
- ³¹P. E. Moroz, in *23rd IEEE Conference on Plasma Science*, Boston, MA (Institute of Electrical and Electronic Engineers, New York, 1996), p. 190.
- ³²P. E. Moroz, D. B. Batchelor, B. A. Carreras, S. P. Hirschman, V. E. Lynch, D. A. Spong, J. S. Tolliver, and A. Ware, "Ultra low aspect ratio stellarator or hybrid configurations," to appear in *Fusion Technol.* (1996).
- ³³S. P. Hirshman and J. C. Whitson, *Phys. Fluids* **26**, 3553 (1983).
- ³⁴S. P. Hirschman and H. K. Meier, *Phys. Fluids* **28**, 1387 (1985).
- ³⁵S. P. Hirschman and D. K. Lee, *Comput. Phys. Commun.* **39**, 161 (1986).
- ³⁶P. E. Moroz, *Phys. Plasmas* **2**, 4269 (1995).
- ³⁷L. M. Kovrizhnykh and P. E. Moroz, *Sov. Phys. Tech. Phys.* **9**, 735 (1983).
- ³⁸A. H. Boozer and G. Kuo-Petravic, *Phys. Fluids* **24**, 851 (1981).
- ³⁹G. Kuo-Petravic and A. H. Boozer, *J. Comput. Phys.* **51**, 261 (1983).
- ⁴⁰S. P. Hirshman, K. C. Shaing, W. I. van Rij, C. O. Beasley, and E. C. Crume, *Phys. Fluids* **29**, 2951 (1986).
- ⁴¹C. D. Beidler, W. N. G. Hitchon, W. I. van Rij, S. P. Hirshman, and J. L. Shohet, *Phys. Rev. Lett.* **58**, 1745 (1987).
- ⁴²D. T. Anderson, A. F. Almagri, F. S. B. Anderson, P. G. Matthews, J. L. Shohet, and J. N. Talmadge, *Bull. Am. Phys. Soc.* **39**, 1601 (1994).
- ⁴³A. H. Boozer, *Plasma Phys. Controlled Fusion* **37**, A103 (1995).
- ⁴⁴L. S. Solov'ev and V. D. Shafranov, in *Reviews of Plasma Physics*, edited by M. A. Leontovich (Consultants Bureau, New York, 1970), Vol. 5, p. 1.
- ⁴⁵R. E. Waltz and A. H. Boozer, *Phys. Fluids B* **5**, 2201 (1993).
- ⁴⁶P. R. Garabedian and H. J. Gardner, *Phys. Plasmas* **2**, 2020 (1995).
- ⁴⁷H. Maassberg, W. Lots, and J. Nührenberg, *Phys. Fluids B* **5**, 3728 (1993).
- ⁴⁸R. J. Bickerton, J. W. Connor, and J. B. Taylor, *Nature Phys. Sci.* **229**, 110 (1971).
- ⁴⁹K. C. Shaing, E. C. Crume, J. S. Tolliver, S. P. Hirshman, and W. I. van Rij, *Phys. Fluids B* **1**, 148 (1989).
- ⁵⁰K. C. Shaing, B. A. Carreras, N. Domingues, V. E. Lynch, and J. S. Tolliver, *Phys. Fluids B* **1**, 1663 (1989).
- ⁵¹K. C. Shaing, S. P. Hirshman, and J. S. Tolliver, *Phys. Fluids* **29**, 2548 (1986).
- ⁵²K. Watanabe, N. Nakajima, M. Okamoto, Y. Nakamura, and M. Wakatani, *Nucl. Fusion* **32**, 1499 (1992).